JOURNAL OF MATERIALS SCIENCE 23 (1988) 2394–2402

Radius of gyration, maximum extensibility and intrinsic crazing in thermoplastics

NICOLE HEYMANS
Physique des Matériaux de Synthèse 194/8, Université Libre de Bruxelles, 1050 Bruxelles, Belgium

An expression for the radius of gyration of a deformed chain is derived, assuming affine deformation of end-to-end vectors defining an entangled length, and random chain behaviour on a shorter scale. This expression is compared with small-angle neutron scattering results from the literature on variation with strain of the radius of gyration. The theoretical variation of the radius of gyration with strain is used to derive an expression for the dependence of limiting glassy-state extensibility on rubbery state pre-strain. This expression is found to give an adequate description of experimental observations of limiting extensibility identified with the critical strain for initiation of intrinsic crazing.

1. Introduction

In an investigation by small-angle neutron scattering (SANS) on polystyrene networks it was found by Benoît *et al.* [1] that although end-to-end vectors joining crosslinks deform affinely, both in uniaxial extension and on swelling, the radii of gyration of chains joining crosslinks do not follow the affine model. Subsequently, similar investigations on polystyrene deformed in the rubbery state [2–5] and on polystyrene [6] and polymethylmethacrylate [7] deformed in the glassy state have confirmed that deformation of the radii of gyration is not uniformly affine. Various interpretations of these observations have been advanced, in terms of two competing deformation modes [2, 4, 6].

An alternative interpretation will be given in this paper, in terms of a single deformation mode: it will be assumed that the random-chain affine model is applicable to any single entangled length. This leads to non-affine deformation of the radius of gyration for short chains, progressively shifting to affine deformation for chains much longer than the entangled length.

It was shown recently that a wide variety of observations on glassy polymers were compatible with a definition of the entangled length as the length of chain required for the reference chain to interact with a constant number of neighbouring chains [8]. One consequence of the non-affine behaviour of the radius of gyration is that a given length of chain interacts with a deformation-dependent number of neighbours; conversely, the deformation dependence of the entangled length can be obtained from that of the radius of gyration. When a polymer is pre-oriented in the rubbery state, the maximum extensibility on subsequently drawing in the glassy state is altered; the maximum extensibility has been interpreted by Dettenmaier and Kausch [9] as the point at which intrinsic crazing appears. It will be shown below that the above-mentioned definition of an entangled length, combined with the calculated variation of the radius of gyration, gives an adequate description of maximum extensibility in polycarbonate (PC), as obtained from observations by Dettenmaier and Kausch [9] and ourselves.

2. Experimental procedure

Dumb-bell shaped specimens having gauge dimensions 40 mm × 8 mm × 2 mm were cut from commercially available PC sheet (Makrolon). They were drawn at 160° C in an Instron tensile tester at various crosshead displacement rates, generally 2 cm min^{-1}. Details of pre-orientation conditions are given in Table I, and the pre-orientation treatment of one sample is shown in Fig. 1. At these strain rates, deformation was not totally reversible. When the required draw ratio was reached, the sample was rapidly cooled at fixed extension by wrapping it in a cloth soaked in icy water. The draw ratio λ_1 was determined as the ratio of cross-sectional areas before and after drawing. (Deformation was not uniform; the samples were distinctly waisted, making measurements of marker displacements difficult to interpret.) Birefringence was measured by compensating with a wedge-shaped sample of drawn PC of known birefringence.

The samples were then drawn at 135° C at a crosshead displacement rate of 2 cm min^{-1}. Initiation of intrinsic crazing was detected optically in transmitted light, and was taken as the point at which the relative decrease in intensity reached 4%. In this manner, initiation of intrinsic crazing could be detected before it became distinctly apparent as a stationary stress on the stress–strain curve. The method is not infallible at low pre-orientations, since surface crazes initiated below yield expanding at high draw ratios also cause a decrease in transmitted intensity; the presence of intrinsic crazing, which gives the samples a distinctive translucent appearance, was checked after unloading. The draw ratio at initiation of intrinsic crazing, λ_2^{II},

0022–2461/88 $03.00 + .12

TABLE I Pre-orientation conditions and draw ratio at initiation of intrinsic crazing

Sample No.	$\dot{l}$ (cm min^{-1})	Δl (cm)	λ_1	$100\Delta n_1$	λ_2	Symbol (Figs 4 to 7)
1	2	See Fig. 1	2.45	0.07	2.02	●–
2	2	2	1.41	0.90	1.85	●
3	2	2	1.52	1.09	1.72	●
4	2	4	2.25	1.63	1.53	●
5	2	6	2.90	1.85	1.47	●
6	2	8	4.27	1.69	1.23	●
7	2	8	3.98	1.99	1.26	●
8	5	4.2	2.22	2.15	1.33	●
9	1	4.1	2.35	1.43	1.53	–●
10	0.5	4	3.81	0.82	1.79	●
11	2	8 – 4	2.59	0.43	1.82	■
12	2	4 – 2	1.64	0.47	1.86	□

was taken as the ratio of cross-sectional areas before and after drawing at 135° C.

Finally, the recoverable draw ratio λ_r was determined after shrinkage at 160° C.

Results are given and discussed in Section 4.2.

3. Theory

3.1. Radius of gyration

3.1.1. Single entangled length: $n = n_e$

3.1.1.1. Individual chain. An appropriate description of deformation will differ, depending on the relevant scale. On a sufficiently large scale, deformation may be assumed uniform, the chain is firmly embedded in the surrounding continuum by interactions with neighbouring chains, and displacements are affine in the macroscopic components. On a smaller scale, the number of neighbours interaction with a given chain decreases, resulting in less efficient restriction of motion; and finally, on a local scale the chain conformation may be assumed random, or at least as random as compatible with large-scale restrictions on conformations. As a first approximation, the intermediate partially restricted state will be ignored, and it will be assumed that a critical number of segments n_e exists, such that for $n < n_e$ chain configuration is random, and that for $n > n_e$ the relative displacement of chain ends is affine; n_e thus defines the entangled length of polymer chain. So far the model is similar to the rubbery elastic model, in which affine behaviour is assumed for end-to-end vectors joining crosslinks, and a random configuration is assumed for the chain between crosslinks. In the present context, however, diffuse entanglements are assumed, so that the "beginning" and "end" of the entangled length can be taken at random anywhere along the chain; in the literature, the term "entanglement length" is usually synonymous with "length between entanglement points" implying localized entanglements, and in this paper the term "entangled length" will be preferred in order to pinpoint the fact that entangling is assumed to be a delocalized phenomenon. The situation is depicted schematically in Fig. 2.

An expression for the radius of gyration will now be derived, following the lines of thought found in Volkenstein [10]. Consider a chain of n_e statistical segments, assumed rigid, connected by $(n_e + 1)$ nodes. The vector coordinate $\boldsymbol{r}_i$ of the ith node with respect to the centre of gravity G is

$$\boldsymbol{r}_i = \boldsymbol{r}_{oi} - \boldsymbol{r}_{og} \tag{1}$$

where subscript o refers to the (arbitrary) origin of coordinates and g to the centre of gravity.

The component of the radius of gyration in an arbitrary direction $0z$ is given by

$$\langle z_i^2 \rangle = \langle (z_{oi} - z_{og})^2 \rangle = \frac{\Sigma z_{oi}^2}{n} - z_{og}^2 \tag{2}$$

Putting the origin at the first node,

$$\boldsymbol{r}_{oi} = \sum_{j=1}^{i} l_j \tag{3}$$

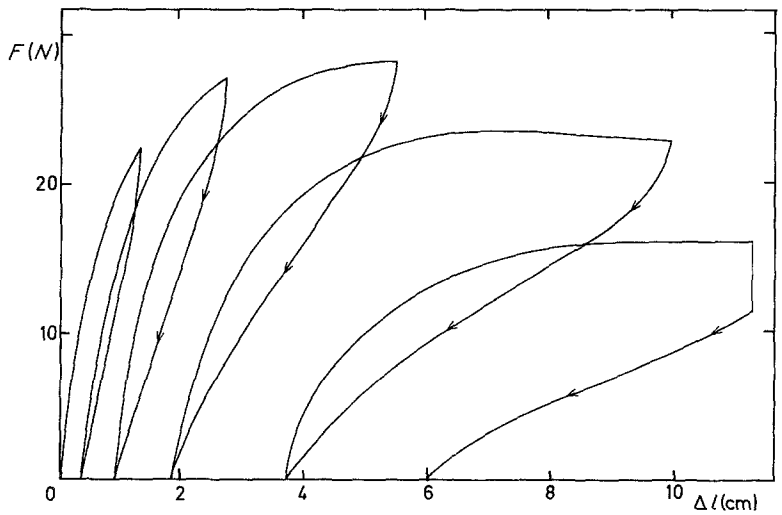

Figure 1 Pre-orientation treatment of Sample 1 (Table I).

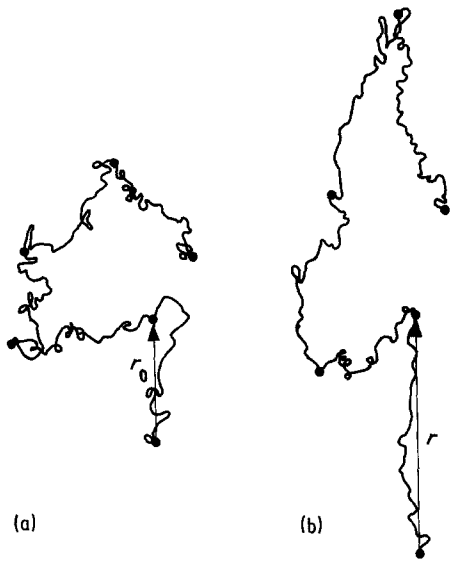

Figure 2 Schematic representation of deformation: (a) relaxed state, (b) deformed state.

where l_j defines the jth bond. If θ_j is the angle between l_j and the arbitrary z direction, the z component of this vector is

$$z_{oi} = \sum_{j=1}^{i} l \cos \theta_j \quad (4)$$

and

$$z_{oi}^2 = \left(\sum_{j=1}^{i} l \cos \theta_j \right)^2 = l^2 \left(\sum_{j=1}^{i} \cos^2 \theta_j + 2 \sum_{j=2}^{i} \cos \theta_j \sum_{k=1}^{j-1} \cos \theta_k \right) \quad (5)$$

The assumption that the chain is free to assume a random configuration means that the various values of θ_j are uncorrelated, so that

$$z_{oi}^2 = l^2 \left(i \langle \cos^2 \theta \rangle + i(i-1) \langle \cos \theta \rangle^2 \right) \quad (6)$$

where the averages are taken over the whole chain. The corresponding coordinate of the centre of gravity is given by

$$z_{og}^2 = \frac{1}{n_e^2} \sum_{i=1}^{n_e} z_{oi} \sum_{j=1}^{n_e} z_{oj} \quad (7)$$

involving products of the form

$$z_{oi} z_{oj} = l^2 \sum_{k=1}^{i} \cos \theta_k \sum_{m=1}^{j} \cos \theta_m \quad (8)$$

$$= l^2 \left[i \langle \cos^2 \theta \rangle + i(j-1) \langle \cos \theta \rangle^2 \right] \quad (9)$$

assuming $i \leqslant j$. Finally:

$$z_{og}^2 = l^2 \frac{(n+1)(2n+1)}{6n} \langle \cos^2 \theta \rangle + \frac{(n+1)(n-1)(3n+2)}{12n} \langle \cos \theta \rangle^2 \quad (10)$$

and, combining Equations 2, 6 and 10,

$$z_i^2 = \frac{n^2 - 1}{6n} l^2 \left[\langle \cos^2 \theta \rangle + \left(\frac{n}{2} - 1 \right) \langle \cos \theta \rangle^2 \right] \quad (11)$$

3.1.1.2. Average radius of gyration. The next step will be to find an expression for the radius of gyration, averaged over the distribution of end-to-end vectors of entangled lengths. $\langle \cos \theta \rangle$ is proportional to the projected length of the end-to-end vector on to the as-yet arbitrary z axis. Let x_p ($p = 1, 2, 3$) define the principal directions of strain, θ_p the segmental orientations with respect to x_p, and let λ_p be the principal draw ratios. As the end-to-end vector deforms affinely,

$$\langle \cos \theta_p \rangle = \lambda_p \langle \cos \theta_{po} \rangle \quad (12)$$

where the subscript o refers to the initial state. If ψ is the angle between a segment and the end-to-end vector (co-latitude), and if the direction cosines of the end-to-end vector are $\cos \alpha_p$,

$$\langle \cos \theta_{po} \rangle = \cos \alpha_{po} \langle \cos \psi_0 \rangle \quad (13)$$

If all entangled lengths are assumed equivalent, $\langle \cos \psi_0 \rangle$ is identical for all chains and is simply the reciprocal of the limit of extensibility λ_M:

$$\cos \psi_0 = 1/\lambda_M \quad (14)$$

$$= n^{-1/2} \quad (15)$$

Also, since the initial distribution of orientations of chains is isotropic,

$$\cos^2 \alpha_{po} = 1/3 \quad (16)$$

giving

$$\langle \cos \theta_p \rangle = \frac{\lambda_p}{\sqrt{3} \times \lambda_M} \quad (17)$$

The average of $\langle \cos^2 \theta_p \rangle$ over all chains is simply the second-order segmental orientation average with respect to direction x_p, and is expandable in terms of second-order Legendre polynomials. From here on attention will be restricted to uniaxial symmetry, in which case these reduce to the second-order spherical harmonic:

$$P_2 = \frac{3\cos^2 \theta - 1}{2} \quad (18)$$

In the case of uniaxial extension with draw ratio λ along the z axis,

$$\langle \cos^2 \theta_z \rangle = \frac{2\langle P_2 \rangle + 1}{3} \quad (19)$$

$$\langle \cos^2 \theta_x \rangle = \langle \cos^2 \theta_y \rangle = \frac{1 - \langle P_2 \rangle}{3} \quad (20)$$

In this case Equation 17 becomes

$$\langle \cos \theta_z \rangle = \lambda / 3^{1/2} \lambda_M \quad (21)$$

$$\langle \cos \theta_x \rangle = \langle \cos \theta_y \rangle = 1/(3\lambda)^{1/2} \lambda_M \quad (22)$$

and finally the contributions to the radius of gyration in directions parallel and perpendicular to the macroscopic strain are

$$R_\parallel^2 = \frac{n^2 - 1}{18n} l^2 \left[2\langle P_2 \rangle + 1 + \left(\frac{1}{2} - \frac{1}{n} \right) \lambda^2 \right] \quad (23)$$

$$R_\perp^2 = \frac{n^2 - 1}{18n} l^2 \left[1 - \langle P_2 \rangle + \left(\frac{1}{2} - \frac{1}{n} \right) \frac{1}{\lambda} \right] \quad (24)$$

In the initial state, since $\langle P_2 \rangle = 0$ when $\lambda = 1$, both equations reduce to

$$R_{po}^2 = \frac{n^2 - 1}{18n} l^2 \left(\frac{3}{2} - \frac{1}{n} \right) \quad (25)$$

and the radius of gyration is then given by

$$R_o^2 = \sum_1^3 R_{po}^2 = \frac{n^2 - 1}{6n} l^2 \left(\frac{3}{2} - \frac{1}{n}\right) \quad (26)$$

Note that this expression is different from the classical result

$$R_g^2 = nl^2/6 \quad (27)$$

because when deriving the classical result $\langle \cos \theta \rangle$ is generally assumed negligibly small for long chains; in fact, although $\langle \cos \theta \rangle$ is of order $n^{-1/2}$, it is involved in n times more terms than $\langle \cos^2 \theta \rangle$ so that finally both terms are of the same order of magnitude in a real chain, however long.

3.1.2. Long chains: $n > n_e$

The condition of uncorrelated angles of rotation will generally not be met when the chain length is larger than the entangled length: for each successive entangled length $\langle \cos \theta \rangle$ will assume the value appropriate for the local chain orientation and draw ratio, rather than the average for the whole chain. The situation may be approximated by assuming the development given in the preceding section to be valid for nodes separated by fewer than n_e bonds, with the additional assumption of affine deformation for nodes separated by more than n_e bonds. The radius of gyration along z is then given by

$$\langle z_i^2 \rangle = \frac{1}{n}\left(\sum_1^{n_e} z_i^2 + \lambda^2 \sum_{n_e+1}^{n} z_{io}^2\right) \quad (28)$$

$$= \frac{\lambda^2}{n}\sum_1^n z_{io}^2 + \frac{n_e}{n}\left(\frac{1}{n_e}\sum_1^{n_e} z_i^2 - \frac{\lambda^2}{n_e}\sum_1^{n_e} z_{io}^2\right) \quad (29)$$

On averaging over all chains, making use of Equation 23, taking account of the fact that when $\lambda = 1$, $\langle P_2 \rangle = 0$, and making the simplifying assumptions $n \gg 1$ and $n_e^2 \gg 1$,

$$\sum_1^n z_{io}^2 = \frac{n^2 l^2}{18}\frac{3}{2} \quad (30)$$

$$\sum_1^{n_e} z_{io}^2 = \frac{n_e^2 l^2}{18}\left(\frac{3}{2} - \frac{1}{n_e}\right) \quad (31)$$

$$\sum_1^{n_e} z_i^2 = \frac{n_e^2 l^2}{18}\left[1 + 2\langle P_2 \rangle + \left(\frac{3}{2} - \frac{1}{n_e}\right)\lambda^2\right] \quad (32)$$

and finally

$$R_\parallel^2 = R_{\parallel o}^2\left[\lambda^2 - \frac{2n_e^2}{3n^2}(\lambda^2 - 1 - 2\langle P_2 \rangle)\right] \quad (33)$$

Use of Equation 23 to obtain Equation 30 although $n > n_e$ is justified by the fact that initially thermal equilibrium is assumed, i.e. the assumptions of random configuration and uncorrelated segmental orientations are initially assumed valid for the whole chain. This might not be justified for very long chains, but in this case deformation of the radius of gyration will be affine whether the initial state is described by Equation 29 or not.

The equivalent expression for $R_\perp^2$ is

$$R_\perp^2 = R_{\perp o}^2\left[\frac{1}{\lambda} - \frac{2n_e^2}{3n^2}\left(\frac{1}{\lambda} - 1 + \langle P_2 \rangle\right)\right] \quad (34)$$

Equations 33 and 34 reduce to the affine expressions when $n \gg n_e$.

3.2. Maximum extensibility

The maximum extensibility of a polymer network is reached when those chains whose end-to-end vectors are aligned with the draw direction are fully stretched; at this point

$$\lambda_M^2 = n_e \quad (35)$$

In this paragraph, the subscript e will be omitted in an effort to improve clarity.

It has been shown that for polymers with widely varying entanglement molecular weights, the ratio of end-to-end distance to average spacing is a universal constant within experimental scatter [8]. Equivalently, the ratio of pervaded to occupied volume is a constant, which may be thought of as an interaction parameter and will be noted k. The implication is that, for a chain to be entangled, it must interact with a minimum number of neighbouring chains. This number must be of the same order of magnitude as k, although of course the reference chain does not interact with all the chains with which it shares the pervaded volume.

If deformation of the radius of gyration is non-affine, the pervaded volume becomes strain-dependent and the entangled length must adjust as deformation proceeds.

The assumption of affine transformation of the coil dimensions in the glassy state has been made previously to obtain a relationship between birefringence and strain [11]; the model was in reasonable agreement with experimental results, and consequently the assumption will be made here that the entangled length is independent of strain in the glassy state, depending solely on the conformation inherited from the melt. On the other hand, when the polymer is deformed in the rubbery state, deformation of end-to-end vectors is affine, but deformation of the radius of gyration is not, resulting in a variation of the entangled length as deformation proceeds.

Consequently, when a polymer has been pre-oriented in the rubbery state, the glassy-state extensibility will subsequently be limited by the most highly stretched chains, which will vary depending on the relative orientation of the rubbery-state and glassy-state extensions λ_1 and λ_2.

First consider λ_2 parallel to λ_1. The chains limiting the glassy-state extensibility will be those whose end-to-end vectors are aligned with the initial draw direction (IDD), z. If, as before, ψ is the co-latitude defining segmental orientation with respect to the end-to-end vector, Equation 11 becomes, for directions z and x respectively parallel and perpendicular to the draw direction,

$$\langle z^2 \rangle = \frac{nl^2}{6}\left(\frac{2\langle P_2(\psi) \rangle + 1}{3} + \frac{\lambda_1^2}{2}\right) \quad (36)$$

$$\langle x^2 \rangle = \frac{nl^2}{6}\left(\frac{1 - \langle P_2(\psi) \rangle}{3}\right) \quad (37)$$

where $\langle P_2(\psi)\rangle$ is the segmental orientation average with respect to the end-to-end vector, and the approximation $n \gg 1$ has been made.

The pervaded volume is assumed proportional to

$$\langle x^2\rangle \langle z^2\rangle^{1/2} = n^{3/2} \tfrac{l^3}{108} (4P_2 + 2 + 3\lambda_1^2)^{1/2} (1 - P_2) \quad (38)$$

whereas the occupied volume is proportional to n, and the interaction parameter is given by the ratio of pervaded to occupied volumes, i.e.

$$k = n^{1/2} \tfrac{1}{108} (4P_2 + 2 + 3\lambda_1^2)^{1/2} (1 - P_2) \quad (39)$$

where P_2 has been substituted for $\langle P_2(\psi)\rangle$.

If the interaction parameter is assumed constant, the variation with strain of the number of statistical segments in an entangled length is

$$n_\parallel = n_0 \frac{(4P_{20} + 5)(1 - P_{20})^2}{(4P_2 + 2 + 3\lambda_1^2)(1 - P_2)^2} \quad (40)$$

The segmental orientation average P_2 is related to the fractional extension of the chain, given by

$$t = \lambda_1/\lambda_M \quad (41)$$

A simple and reasonable assumption is to use Treloar's approximation for the orientation average resulting from the Langevin distribution:

$$P_2 = 0.6t^2 + 0.2t^4(1 + t^2) \quad (42)$$

The adequacy of this relationship has been demonstrated, even for quite small values of n [12]. Equation 40 is now an implicit equation, which can easily be solved for n by an iterative procedure. The limit of extensibility in the glassy state is finally

$$\lambda_{2M\parallel} = n_\parallel^{1/2}/\lambda_1 \quad (43)$$

Now consider the case when the glassy-state extension is in a direction (e.g. x) perpendicular to the IDD (z). The chains limiting glassy-state extensibility are now those whose end-to-end vector is aligned with the x axis. Deformation is no longer transverse isotropic with respect to the x direction; however, the basic assumption in this work is that, in the rubbery state, deformation of end-to-end vectors defining an entangled length is affine in the macroscopic deformations, and that on any shorter scale the chain configuration is as random as is compatible with this constraint. As transverse dimensions are smaller than the end-to-end length, it seems more reasonable to assume transverse isotropy of the components of the radius of gyration than to assume them to be proportional to macroscopic deformations. Under the assumption of transverse isotropy of chain dimensions, λ_1^2 must simply be replaced by $1/\lambda_1$, and Equations 40 and 43 then become

$$n_\perp = n_0 \frac{(4P_{20} + 5)(1 - P_{20})^2}{[4P_2 + 2 + (3/\lambda_1)](1 - P_2)^2} \quad (44)$$

$$\lambda_{2M\perp} = (n_\perp \lambda_1)^{1/2} \quad (45)$$

where P_2 is related to the fractional extension $(n_\perp \lambda_1)^{-1/2}$. Note that Equations 40 and 45 predict anisotropy of the entangled length, depending on the glassy-state stretching direction; the common assumption of a gradual breakdown of the entanglement network as deformation proceeds does not allow for such anisotropy, so that comparisons of maximum extensibility perpendicular and parallel to the IDD should discriminate between the two assumptions. In fact, as will be shown below, this comparison is somewhat inconclusive in the case of polycarbonate.

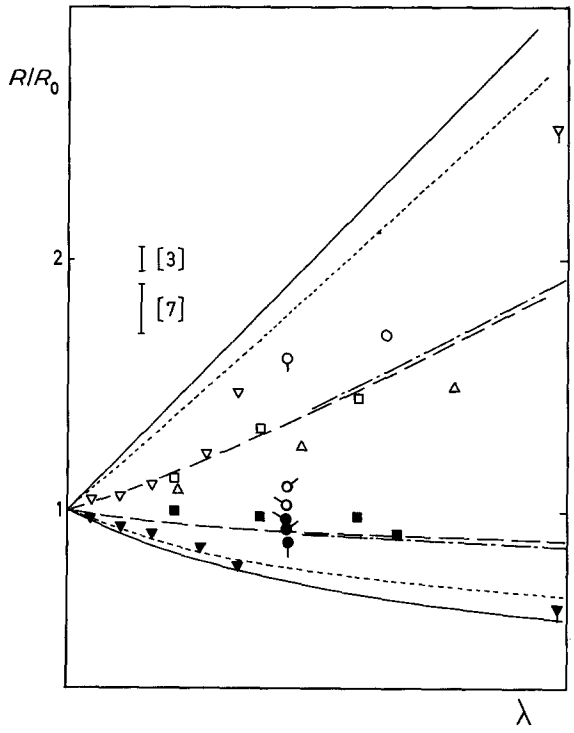

Figure 3 Variation of radius of gyration with strain. Curves: (——) affine model; (– –) Equations 23 and 24 with $n = 25$, $P_2 = 0$; (–·–·–) the same with P_2 from Equation 46; (– – –) Equations 33 and 34, $P_2 = 0$, $n = 2n_e$. Experimental points: (△) PS, swollen network, $M = 26\,000$ (from [1]); (▽, ▼) PS, $M_w = 1.2 \times 10^5$, uniaxial extension, 120° C (from [2]); (▽, ▼) the same at 110° C; (□, ■) PS network, $M = 25\,000$ (from [3]); (○, ●) PS, $M_w = 1.2 \times 10^5$, uniaxial extension, 110° C (from [4]); (○, ◐) the same after 1800 sec relaxation; (◑, ●) the same after 10 800 sec relaxation; (○) PMMA, $M_w = 6000$ blended with $M_w = 23 \times 10^4$, uniaxial extension, 100° C (from [7]). Open symbols: parallel to strain, closed symbols: perpendicular to strain.

Note also that, for polymers with a large initial entangled length (i.e. small P_{20}), the effect of the increase in strain, leading to an increase in the longitudinal radius of gyration, will predominate over the decrease in the transversal radius of gyration ($(1 - P_2)$ will remain close to unity) at low to moderate strains, so that in fact the model predicts a decrese in maximum extensibility at moderate pre-strains. This is difficult to check experimentally, as polymers with a large entangled length tend to craze and are usually brittle in the glassy state.

4. Comparison with experiment

4.1. Radius of gyration

Experimental results from various sources are compared with the predictions of the model developed in Section 3.1.1.1 (Equations 23 and 24) and with those of the affine model in Fig. 3. In Equations 23 and 24, n was set equal to 25, corresponding to a limiting extension of 5, and $\langle P_2\rangle$ was set equal to zero (dashed lines) or to the rubbery-elastic theoretical value

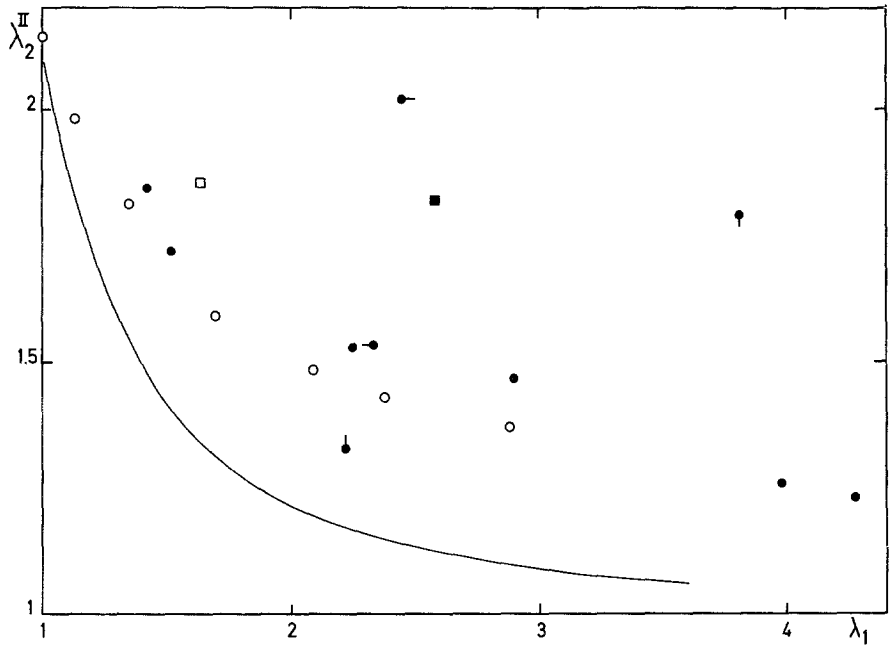

Figure 4 Draw ratio at initiation of intrinsic crazing against apparent draw ratio after pre-orientation at 160° C. 135° C, this work: see Table I for symbol key; (○) 129° C from [9]; (——) from Equation 40 with $n_0 = 4.4$.

resulting from integration of Equation 42 (dashed-dotted line), i.e.

$$\langle P_2 \rangle = \frac{1}{15n}\left(\lambda^2 - \frac{1}{\lambda}\right) + \frac{1}{75n^2}\left(\lambda^4 + \frac{\lambda}{3} - \frac{4}{3\lambda^2}\right) + \frac{1}{105n^3}\left(\lambda^6 + \frac{3\lambda^3}{5} - \frac{8}{5\lambda^3}\right) \quad (46)$$

These predictions are largely insensitive to changes in n.

The dotted lines are calculated from Equations 33 and 34, with $\langle P_2 \rangle = 0$ and $n = 2n_e$. The results obtained by Maconnachie *et al.* [4] on polystyrene (PS) undergoing stress relaxation have been plotted in Fig. 3 as the ratio of $R_\perp$ and $R_\parallel$ to the final isotropic radius of gyration, which was slightly larger than the initial value. The draw ratio was taken as the macroscopic, or effective, draw ratio (determined from changes of dimensions), although it would be more appropriate to use the molecular draw ratio determined from shrinkage.

Comparison between theory and experiment is somewhat obscured by experimental scatter, indicated by the error bars (when given). It is interesting to note, however, that the theory predicts near-affine behaviour for chains of only twice the entangled length, although experimental deviations from affine behaviour are large, even for chains which are much longer than the entangled length determined from melt elasticity ($M_e = 18\,100$), or the critical molecular weight from viscosity measurements ($M_c = 31\,200$), but are interestingly rather close to the critical molecular weight at which the compliance determined in creep recovery becomes independent of molecular weight ($M_c' = 130\,000$) (Values for PS are taken from Table 5.2 in Graessley [13]). In terms of the present model, this could mean that M_c' characterizes the scale at which deformation is affine, and M_e the scale below which random-chain behaviour sets in. M_e can be thought of as a mathematical artefact obtained by identifying the low-strain behaviour of an entangled melt with that of an ideal rubbery network. If the entanglement effect is indeed distributed along the chains as hypothesized here, the number of available conformations for a given length of chain is reduced as compared with the random chain, giving an increased modulus and lower apparent entanglement molecular weight: absolute values of entanglement molecular weight should be treated with caution, although variations between polymers can be accepted as real, since M_e and M_c are generally in a constant ratio.

The results of Hadzioannou *et al.* [5], obtained on PS with $M_w = 5.4 \times 10^5$ at draw ratios between 2.9 and 9.4 (not represented in Fig. 3), indicate near-affine transformation of radii of gyration at draw ratios up to 5, becoming slightly non-affine at the highest draw ratio, i.e. 9.4. Clearly, this molecular weight is much larger than the critical molecular weight at which deformation becomes affine.

The results of Dettenmaier *et al.* [7] on high-molecular weight polymethylmethacrylate (PMMA) ($M_w = 1.7 \times 10^5$ and 2.5×10^5), also omitted from Fig. 3 for clarity, demonstrate that, in this range of M_w, variation of R_g is affine in the macroscopic draw ratio, within experimental error.

In summary, measurements of radii of gyration of short chains against draw ratio lend support to the model presented here, in which long-scale deformation is assumed affine and the random-chain approximation is applied on a local scale.

4.2. Maximum draw ratio

The draw ratio of pre-oriented samples at initiation of intrinsic crazing is plotted in Fig. 4 against apparent draw ratio λ_1 after pre-orientation, together with results obtained by Dettenmaier and Kausch [9] on Makrolon under similar conditions. The theoretical curve is calculated from Equation 39, putting $n_0 = 4.4$ (i.e. $\lambda_M = 2.1$ for the unoriented polymer). Although the results of Dettenmaier and Kausch follow a smooth curve, the results obtained in this laboratory exhibit wild scatter, depending on sample preparation. The results of Dettenmaier and Kausch [9] obtained on samples pre-oriented at a strain rate of 200% min^{-1} appear to set an approximate lower limit to our own, obtained on samples pre-strained at lower strain rates,

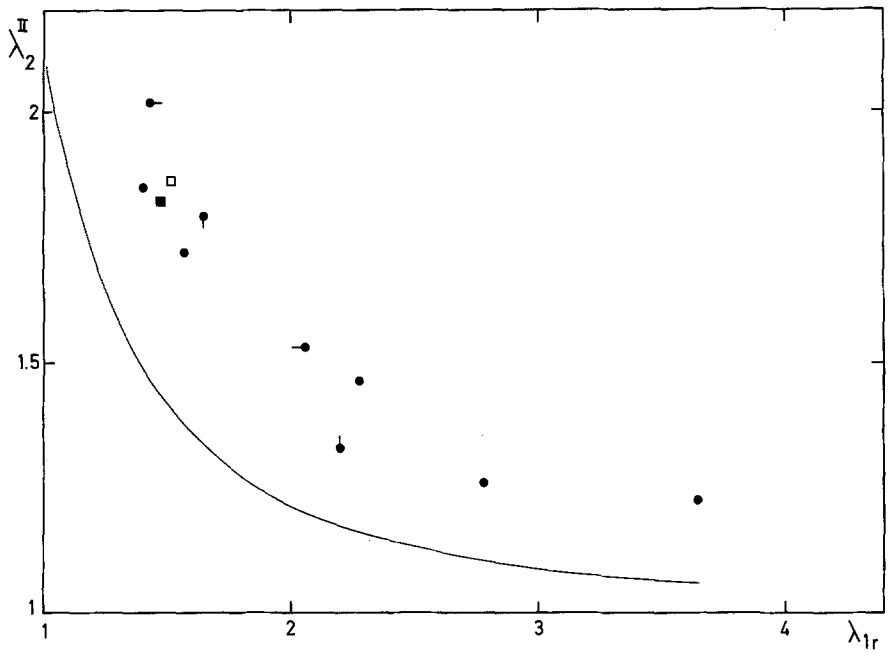

Figure 5 Draw ratio at initiation of intrinsic crazing against recoverable draw ratio determined after shrinkage at 160° C. Symbols as in Fig. 4.

and all results lie above the theoretical predictions. The points which lie furthest from the theoretical predictions correspond to the samples which had spent the longest times under strain at 160° C. This suggests that the pre-strain might include a non-recoverable component: the maximum strain given by Equation 40 is defined with respect to the isotropic relaxed state; the appropriate draw ratio is therefore the recoverable draw ratio λ_r determined after shrinkage.

The draw ratio at the onset of intrinsic crazing λ_2^{II} is plotted in Fig. 5 against the recoverable pre-strain λ_{1r}, defined as λ_r/λ_2^{II}. The underlying hypothesis is that recovery of deformation undergone at 135° C is complete at 160° C, which is indeed the case for unoriented samples, and that irrecoverable deformation is linked only with pre-orientation conditions. Some scatter remains, although it is now greatly reduced. (The results of Dettenmaier and Kausch have been omitted from Fig. 5, as no shrinkage data were available). The remaining scatter is probably traceable to difficulties in choosing the appropriate shrinkage time: shrinkage at 160° C is initially very fast, but after a couple of minutes the shrinkage rate decreases considerably and finally becomes negligible after approximately half an hour. At this point, recovery is generally far from complete, particularly for samples which had been pre-strained at low strain rates or submitted to complicated loading histories. The steady-state value of λ_r was used here, although it might have been more appropriate to take the value corresponding to immediate recovery.

Scatter is further reduced when λ_2^{II} is plotted against Δn_1, the birefringence measured at room temperature after pre-orientation (Fig. 6). This suggests that the appropriate pre-strain may be correlated with birefringence. In Fig. 7, λ_2^{II} is plotted against values of pre-strain obtained from the relationship between birefringence and strain measured in creep at 130° C (Fig. 8). (This relationship is extremely close to the results of Dettenmaier and Kausch [9] at 129° C.) This procedure probably underestimates λ_1, as birefringence in the glassy state is known to include a temperature-dependent contribution [11] which probably only vanishes at the glass transition [15]. The limiting draw ratio now lies below (or to the left of) the theoretical prediction, confirming this interpretation.

To check the internal consistency of the model, the results of Dettenmaier and Kausch [9] on samples drawn in the glassy state in a direction perpendicular to the IDD are compared in Table II with those obtained with λ_2 parallel to the IDD. In their work, the results are presented as λ_2^{II} against Δn_1 ([9], Fig. 7) and, for λ_2 parallel to λ_1, as $\ln \lambda^{II}$ against λ_1 (Fig. 8) where λ^{II} is the total draw ratio at initiation of intrinsic crazing, i.e. $\lambda_1\lambda_2^{II}$. In Table II, only those results obtained on samples with comparable initial draw ratios for both subsequent draw directions are given. Draw ratios at the initiation of intrinsic crazing are those directly read from [9], Fig. 7. For λ_2 parallel to

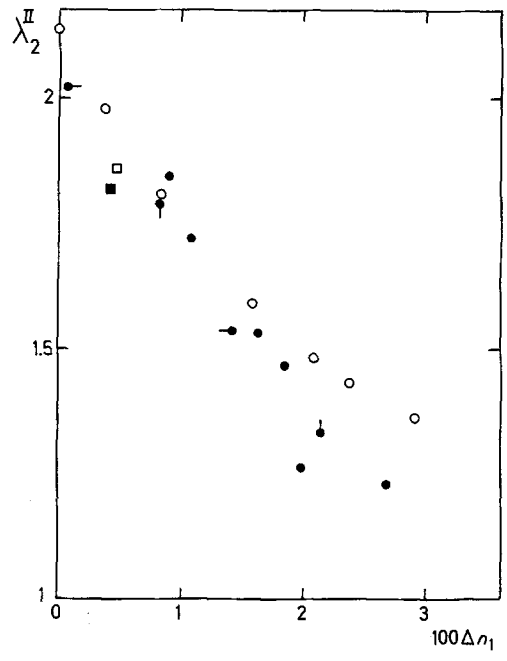

Figure 6 Draw ratio at initiation of intrinsic crazing against birefringence measured after pre-orientation. Symbols as in Fig. 4.

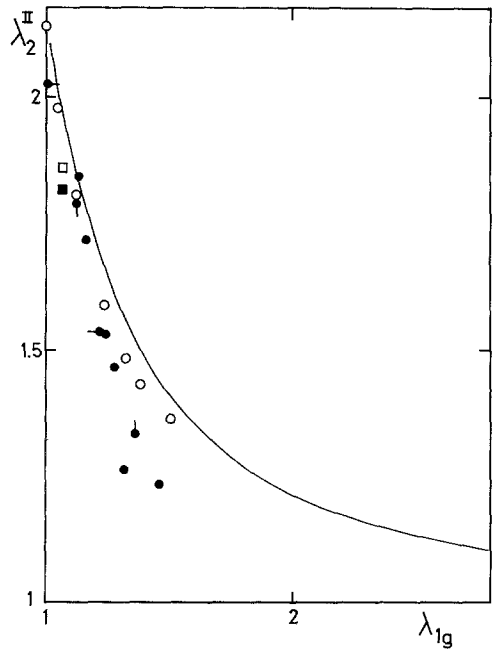

Figure 7 Draw ratio at initiation of intrinsic crazing against draw ratio obtained from birefringence and Fig. 8. Symbols as in Fig. 4.

λ_1, the apparent draw ratio λ_1 is obtained from [9], Fig. 8; for λ_2 perpendicular to λ_1 it is obtained by interpolation using the value of Δn_1 read from their Fig. 7 and the relationship between Δn_1 and λ_1 obtained by eliminating λ_2^{II} (parallel to λ_1) between Figs 7 and 8 of [9].

Equations 40 and 44 give a relationship between λ_M and λ_1 which can be used to obtain a correspondence between λ_2^{II} and λ_1, assuming that initiation of intrinsic crazing occurs when the network reaches the maximum draw ratio, i.e.

$$\lambda_2^{II} = \lambda_M/\lambda_1 \qquad \lambda_2 \parallel \lambda_1 \tag{47}$$

$$\lambda_2^{II} = \lambda_M \lambda_1^{1/2} \qquad \lambda_2 \perp \lambda_1 \tag{48}$$

Conversely, the experimental values of λ_2^{II} can be used to obtain the corresponding theoretical value of λ_1, called λ_{1c} in Table II. Also, a "glassy state" value λ_{1g} can be obtained from the experimental value of Δn_1

TABLE II Comparison between models for glassy-state limit of extensibility

λ_1 (ADR) [9]	1.13	1.14	1.35	1.38	2.38	2.39
$\lambda_{2\parallel}$ [9]	1.98		1.81		1.43	
$\lambda_{2\perp}$ [9]		2.20		2.26		2.60
$100\Delta n_1$ [9]	0.38	0.41	0.84	0.89	2.38	2.39
λ_{1c} (Equations 40, 44)	1.06	1.10	1.16	1.16	1.47	1.53
λ_{1g} ([9], Fig. 6)	1.06	1.07	1.11	1.12	1.39	1.39
λ_{1e} (Equation 49)	1.07		1.16		1.49	

and from the experimental relationship between birefringence and strain obtained at 129° C ([9], Fig. 6). Lastly, if the limiting strain is assumed to be determined by the average "entanglement density", a third value, called λ_{1e}, can be calculated as

$$\lambda_{1e} = (\lambda_{2\perp}^{II}/\lambda_{2\parallel}^{II})^{2/3} \tag{49}$$

Values of λ_{1c} and λ_{1e} are quite close to each other, because in fact Equations 40 and 44 predict only a small variation of maximum extensibility in this range of pre-strains. Agreement between values of λ_{1c} for λ_2 parallel and perpendicular to the IDD is also fair, and can be improved by adjusting the maximum extensibility of the isotropic material, i.e. by assuming that intrinsic crazing occurs slightly below the limiting extensibility. This adjustment is not carried out here, as it requires definition of a parameter (the ratio λ^{II}/λ_M) which is not accessible to experiment. The assumption that λ^{II} is identical to λ_M essentially leaves the model with no free parameters.

The results of Dettenmaier and Kausch [9] therefore do not discriminate clearly between the model presented in this paper and the simpler assumption of a constant "entanglement density". (This confirms the previous conclusion that, in a variety of applications, diffuse entanglements can be approximated by the temporary network model [8].) Both models, however, give values of pre-strain which are much lower than the apparent pre-strain, and which are not far removed from those obtained from the glass-state strain corresponding to the experimentally observed birefringence. Again, this seems to be an indication that only part of

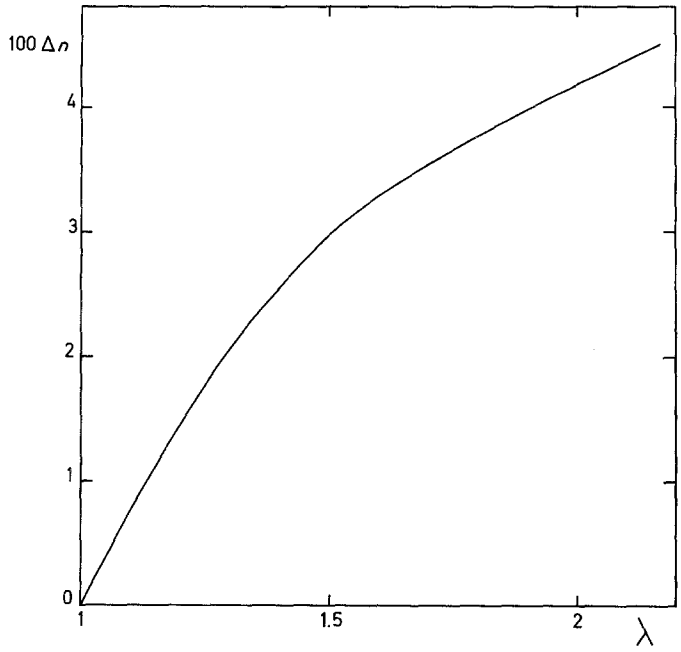

Figure 8 Relation between birefringence and strain in PC at 130° C.

the rubbery strain is effective in determining subsequent glassy-state behaviour. A possible interpretation of this observation is that, on pre-orientation in the rubbery range, rearrangements involve chain lengths larger than the instantaneous entangled length, which determines immediate recovery on unloading in this range, and also subsequent glassy-state behaviour. Long-term recovery is determined by larger-scale rearrangements, and permanent deformation involves the whole chain. More experimental work is required to clarify this point.

Another point deserving clarification is the prediction of Equation 39 that, on low strains, the entangled length should decrease with increasing strain for λ_2 parallel to λ_1, particularly for large initial entangled lengths. This occurs because $(1 - P_2)$ remains close to unity at low strains, and the effect of the increase in end-to-end length is then dominant in determining the pervaded volume. This effect is not large in PC where orientation increases rapidly because of the short entangled length, but should be more visible in polymers such as PS having a larger initial maximum extensibility.

5. Conclusions

A model of chain deformation has been given, in which configuration is assumed random on a local scale, and deformation is assumed affine on a sufficiently large scale. The resulting deformation of the radius of gyration is affine for long chains and less than affine for short chains, in agreement with experimental data by SANS from the literature. Non-affine transformation of the radius of gyration of an entangled length implies a change of the glassy-state maximum extensibility after pre-orientation which is compatible with experimental results on PC, although the possibility of a constant entanglement density cannot be ruled out. There is certainly no experimental support in this case for the common assumption of a breakdown of the entanglement network at high pre-strains.

References

1. H. BENOÎT, D. DECKER, R. DUPLESSIX, C. PICOT, P. REMPP, J. P. COTTON, B. FARNOUX, G. JANNINK and R. OBER, *J. Polym. Sci., Polym. Phys. Edn* **14** (1976) 2119.
2. C. PICOT, R. DUPLESSIX, D. DECKER, H. BENOÎT, F. BOUÉ, J. P. COTTON, M. DAOUD, B. FARNOUX, G. JANNINK, M. NIERLICH, A. J. de VRIES and P. PINCUS, *Macromolecules* **10** (1977) 436.
3. S. B. CLOUGH, A. MACONNACHIE and G. ALLEN, *ibid.* **13** (1980) 774.
4. A. MACONNACHIE, G. ALLEN and R. W. RICHARDS, *Polymer* **22** (1981) 1157.
5. G. HADZIIOANNOU, L.-H. WANG, R. S. STEIN and R. S. PORTER, *Macromolecules* **15** (1982) 880.
6. J. M. LEFEBVRE, B. ESCAIG and C. PICOT, *Polymer* **23** (1982) 1751.
7. M. DETTENMAIER, A. MACONNACHIE, J. S. HIGGINS, H. H. KAUSCH and T. Q. NGUYEN, *Macromolecules* **19** (1986) 773.
8. N. HEYMANS, *J. Mater. Sci.* **21** (1986) 1919.
9. M. DETTENMAIER and H. H. KAUSCH, *Colloid Polym. Sci.* **259** (1981) 937.
10. M. V. VOLKENSTEIN, "Configurational Statistics of Polymeric Chains" (Interscience, Wiley, New York, 1963) p. 180.
11. N. HEYMANS, *Polymer* **28** (1987) 2009.
12. *Idem, ibid.* **27** (1986) 1177.
13. W. W. GRAESSLEY, "The Entanglement Concept in Polymer Rheology", Advances in Polymer Science Vol. 16 (Springer, Berlin, 1974).
14. M. DETTENMAIER and H. H. KAUSCH, *Polymer* **21** (1980) 1232.
15. M.-S. S. WU, *J. Appl. Polym. Sci.* **32** (1986) 3263.

Received 3 June
and accepted 22 September 1987